

Data report: early to middle Eocene benthic foraminifers at Sites U1331 and U1333, equatorial central Pacific Ocean, Expedition 320/321¹

Ritsuo Nomura,² Hiroyuki Takata,³ and Akira Tsujimoto²

Chapter contents

Abstract	1
Introduction	1
Methods	2
Results	2
Early and middle Eocene benthic foraminiferal assemblages	3
Acknowledgments	4
References	4
Appendix	6
Figures	8
Tables	10
Plates	14

Abstract

Benthic foraminiferal assemblages were studied in 44 samples from lower and middle Eocene sediments in Integrated Ocean Drilling Program (IODP) Expedition 320 Holes U1331C, U1333A, and U1333B. The benthic foraminifers from Hole U1331C were sampled in lower Eocene calcareous nannofossil Zones NP12/NP13 and radiolarian Zones RP8/RP9, and thus fall within the early Eocene climatic optimum and those from Holes U1333A and U1333B fall in the upper lower Eocene and lower middle Eocene calcareous nannofossil Zones NP15–NP17 and radiolarian Zones RP13–RP16. The benthic foraminiferal assemblages from Hole U1331C are poorly preserved, so the paleoceanographic response of the benthic assemblage to warming could not be clearly observed. The diversity of benthic assemblages in the middle Eocene is positively correlated with the carbonate content of the samples. The species *Globocassidulina globosa*, which has been argued to be an opportunistic species, occurred in the high-carbonate intervals. Diversities decreased coeval with an increase in abundance of radiolarians, occurring between Sections 320-U1333A-16X-5 and 16X-6, at the time of deposition of the marked carbonate poor horizon in the middle Eocene.

Introduction

Development of Cenozoic benthic foraminiferal assemblages after the prominent extinction during the Paleocene/Eocene Thermal Maximum (PETM; ~56 Ma) has been correlated to periods of global cooling and associated changes in oceanic environments (Kennett and Stott, 1991; Thomas, 2007). Before development of Antarctic ice sheets during the major global cooling at the end of the Eocene, however, several smaller hyperthermals occurred following the PETM, culminating in the early Eocene climatic optimum (EECO, ~52 Ma). These smaller hyperthermals resemble the PETM in geochemical and biotic features (Lourens et al., 2005; Agnini et al., 2009; Zachos et al., 2010; Stap et al., 2010).

Deep-sea benthic foraminifers thus experienced severe climatic fluctuations during latest Paleocene to middle Eocene times. The cause of the benthic extinction during the PETM is still not fully understood, but one convincing explanation could be the change in adaptive strategy of the benthic foraminifers to changes of benthic-pelagic coupling as recognized in the modern ocean (Goody, 2005).

¹Nomura, R., Takata, H., and Tsujimoto, A., 2013. Data report: early to middle Eocene benthic foraminifers at Sites U1331 and U1333, equatorial central Pacific Ocean, Expedition 320/321. In Pälike, H., Lyle, M., Nishi, H., Raffi, I., Gamage, K., Klaus, A., and the Expedition 320/321 Scientists, *Proc. IODP, 320/321*: Tokyo (Integrated Ocean Drilling Program Management International, Inc.). doi:10.2204/iodp.proc.320321.212.2013

²Shimane University, 1060 Nishikawatsu-cho, Matsue, Shimane 690-8504, Japan. Correspondence author: nomura@edu.shimane-u.ac.jp

³BK21 Coastal Environmental System School, Division of Earth Environmental System, Pusan National University, Busan 609-735, Korea.



2003; Thomas, 2007), possibly due to changes in temperature and thus metabolic rates, which could have led to the expansion of the trophic resource continuum (D'haenens et al., 2012), which also related to the global change in ocean ventilation, oxygenation, and productivity (Winguth et al., 2012). Changes in climatic-related oceanic productivity and export productivity thus could have strongly influenced benthic foraminiferal assemblages, and investigating the mode and tempo of the development of early to middle Eocene benthic assemblages may significantly add to our understanding of the mechanisms of paleoceanographic and biotic co-evolution.

Integrated Ocean Drilling Program (IODP) Expedition 320 and Ocean Drilling Program (ODP) Leg 199 (Pacific Equatorial Age Transect [PEAT]) provided unique paleoceanographic information that will be useful for the further development of an orbitally tuned geological timescale because the sites were well placed to obtain information along gradients in paleolatitude, paleodepth, and paleoproductivity. Eocene carbonate-rich sediments were recovered and used to recognize and define carbonate accumulation events (CAE) (Lyle et al., 2005; Pälike et al., 2009). These sites also allowed reconstruction of changes in the carbonate compensation depth (CCD) over time (Pälike et al., 2009), allowing us to test whether there were correlations between biotic evolution and the oceanic carbonate cycle (Griffith et al., 2010).

This report continues our description of lower Eocene benthic foraminifers from ODP Leg 199 Sites 1215, 1220, and 1221 (Nomura and Takata, 2005). The benthic assemblages at IODP Sites U1331 and U1333 at abyssal paleodepths are comparable to those at ODP Sites 1215, 1220, and 1221, also in the abyssal zone (~3000 m paleodepth). These results are very significant to adding to further information from the deeper ocean (Fig. F1).

Methods

Four samples from CaCO₃-rich sediments from Sections 320-U1331C-17H-3 and 17H-4, 31 samples from Sections 320-U1333A-16X-1 to 20X-2, and 9 samples from Sections 320-U1333B-19X-1 to 20X-3 were analyzed. All samples extended over 2 cm of core and were from the few levels in the lower Eocene and lower middle Eocene where carbonate-rich sediments were present (Pälike et al., 2009).

Samples were dried at 70°–80°C overnight and then weighed. Dried sediment samples were treated with 3% hydrogen peroxide solution overnight and

washed through a 63 µm nylon mesh sieve. The residue was then dry-sieved over a 149 µm sieve, and foraminifers were picked from aliquots of the >149 µm size fraction. Because of low abundances of foraminifers in some sections, the numbers of foraminifers counted was less than 200 individuals in some samples. All picked foraminifers were arranged on an assemblage slide for identification of species. The diversity and equitability of the assemblages were estimated using the Shannon-Wiener index. The main source of foraminiferal systematics is Loeblich and Tappan (1988), which compiled well-known works of Plummer (1926), Cushman and Jarvis (1932), Cushman (1946, 1951), and Brotzen (1948). We examined the systematic works of Tjalsma and Lohmann (1983), van Morkhoven et al. (1986), and Jones (1994) for the cosmopolitan deep-sea foraminifers and Kaminski and Gradstein (2005) for the paleogene agglutinated foraminifers.

Results

Hole U1331C

A total of 29 benthic foraminiferal taxa were recognized (Table T1). Preservation of benthic foraminifers at Site U1331 is poor due to diagenesis caused by circulation of pore waters through the underlying basalt. Calcareous forms were poorly preserved, with recrystallized walls. The number of foraminifers per gram of sediment ranges from 1 to 7, very low numbers compared to normal deep-sea sediments. Foraminifers that do not use carbonate to agglutinate such as *Ammovertellina prima*, *Thalmanammina conglobata*, *Paratrochamminoides olszewskii*, and *Cyclamina elegans* occurred mainly in the lower samples studied. It is not clear whether these forms are present because of the shallow CCD or because of local influences. The East Pacific CCD in the early Eocene was located at a relatively shallow depth of 3000–3500 m. The early Eocene paleodepth of Site U1331 was near this CCD but was slightly above the CCD (Pälike et al., 2009).

The most common calcareous forms, *Nuttallides truempyi*, *Oridorsalis umbonatus*, *Anomalinoidea spissiformis*, and *Quadratobulimina pyramidalis*, appeared only in the uppermost sample studied. This assemblage is similar to the normal deep-sea assemblage in the early to early middle Eocene, although it has very low species richness.

Hole U1333A

A total of 79 foraminiferal taxa were recognized in this hole (Table T2). The preservation of benthic for-

aminifers was generally moderate, with recrystallization of the walls in the lower samples, but poor preservation and corroded walls as well as low abundance in the upper interval from Samples 320-U1333A-16X-1, 24–27 cm, through 16X-4, 75–77 cm. The absolute abundance (number of foraminifers per gram of sediment) fluctuates, being higher in the two higher intervals from Samples 320-U1333A-16X-6, 75–77 cm, to 17X-5, 75–77 cm, and 19X-3, 125–127 cm, to 20X-3, 25–27 cm. The former yields 12.9 individuals per gram, and the latter yields 31.8 individuals per gram. A distinct decrease in species number is recognized between Samples 320-U1333A-16X-5, 75–77 cm, and 16X-6, 75–77 cm, decreasing from 27 to 11 taxa. In general, the number of foraminifers per gram of sediment is negatively correlated with the abundance of radiolarians and positively correlated with the carbonate content, with highest numbers during the middle Eocene carbonate accumulation events (CAE 2–3). The species diversity changes from 3.0–4.0 to 0.7–3.0 and the species equitability changes from 0.5–0.6 to 0.7–0.9 between samples with low and high carbonate content. Although a distinct change in species diversity and equitability occurred, the main constituents of the assemblage did not change, suggesting that the decreased abundance is due to dilution with radiolarians rather than dissolution. Agglutinated foraminifers were common in abundance.

The most common species are *Karreriella subglabra*, *Spiroplectammina spectabilis*, *Abyssamina quadrata*, *Alabamina dissonata*, *A. spissiformis*, *Cibicidoides eoceanus*, *Cibicidoides grimsdalei*, *Gyroidinoides girardanus*, *N. truempyi*, *O. umbonatus*, *Siphonodosaria aculeata*, pleurostomellids, and species of *Pullenia*.

Hole U1333B

A total of 67 taxa were recognized in the nine samples studied from Hole U1333B (Table T3). The assemblage in Samples 320-U1333B-20X-1, 73–75 cm, to 20X-2, 73–75 cm, is similar to that recognized in Samples 320-U1333A-19X-4, 25–27 cm, to 20X-1, 25–27 cm, with abundant foraminifers per gram of sediment. In general, the preservation is moderate to poor, and specimens have recrystallized walls.

The foraminiferal species are similar to these in Hole U1333A, including *C. grimsdalei*, *C. eoceanus*, *A. dissonata*, *A. quadrata*, *A. spissiformis*, *G. girardanus*, *N. truempyi*, *O. umbonatus*, and nodogenerinids. Most have large tests with thick walls. The assemblage shows a similar level of species diversity, 3.0–4.0, and similar levels of species equitability, 0.5–0.7.

Early and middle Eocene benthic foraminiferal assemblages

Because of the poor preservation of foraminifers in Hole U1331C and the fact that we found foraminifers in four samples only, we could not observe evidence of any foraminiferal response to the EECO. Carbonate-free agglutinated foraminifers such as *Thalmanammina* and *Cyclammina* occurred only in the lower Eocene, but they are not diagnostic of this climatic optimum (Kaminski and Gradstein, 2005). Rather, they indicate the presence of carbonate-corrosive deep water, as also suggested by the occurrence at other sites of Eocene radiolarian ooze and low-carbonate sediments (Shipboard Scientific Party, 2002). In the early Eocene, Hole U1331C was above the CCD (Pälike et al., 2009), but the common occurrence of the agglutinated taxa indicates that this site did not present a good habitat for calcifying foraminifers or these forms did live there but were not preserved, possibly due to circulation of hydrothermal fluids through the underlying basalts. The lowermost Eocene calcareous sediments directly above the basement basalt contain zeolitic clays formed by such hydrothermal circulation (Pälike et al., 2009). However, sediments further away from the basement basalt are less influenced by hydrothermal activity; thus, the calcareous assemblage could be preserved as seen in Sample 320-U1331C-17H-3, 78–80 cm, with *N. truempyi*, *O. umbonatus*, *A. spissiformis*, and *A. quadrata*. These species are also major constituents of assemblages occurring after the Paleocene/Eocene benthic extinction at Site 1220, near Hole U1331C (Nomura and Takata, 2005). However, the assemblage in Hole U1331C differs from that of Site 1220 in having lower species diversity. The most common species at Site 1220 include *Bulimina bradburyi*, *Bulimina trihedra*, *Globocassidulina globosa*, *Pleurostomella paleocenica*, *Pullenia subcarinata*, *Quadriformina profunda*, *Tappanina selmensis*, and small-sized *Valvalabamina*, but these are not as common in the assemblage in Hole U1331C.

Except for the low-diversity Samples 320-U1333A-16X-1, 25–27 cm, to 16X-5, 75–77 cm, foraminifers in both holes at Site U1333 show almost the same assemblage, characterized by common cosmopolitan species such as *N. truempyi*, *C. grimsdalei*, *C. eoceanus*, and *O. umbonatus*. Their distribution in core sections shows a prominent foraminiferal occurrence at ~200 revised meters composite depth (rmcd) (Fig. F2), which may indicate correlation to either the CAE 2 (47.9–46.9 Ma) or CAE 1 (45.9–44.2 Ma) event. How-

ever, the age of the highest foraminiferal samples and correlation to CAE 2 or CAE 1 is uncertain, with nannofossil datums indicating the age of ~200.0–200.4 rncd at ~45–47 Ma (Westerhold et al., 2012), with both CAE 1 and CAE 2 occurring within this time interval. A distinct decrease in foraminiferal abundance between Sections 320-U1333A-16X-5 and 16X-6 (174.1–175.5 rncd) occurring in Magneto-chron C18r is correlated with CAE 3, which occurred also in Magneto-chron C18r. CAE 3 is associated with shallowing of the CCD at the end of the event (Lyle et al., 2005).

Acknowledgments

We thank R. Kawagata, Yokohama National University, for his helpful advice on nodosariid and pleurostomellid foraminiferal taxonomy. We appreciate E. Thomas for her constructive review and T. Westerhold, University of Bremen, for providing composite depth data at the studied site. This research used samples provided by the Integrated Ocean Drilling Program (IODP).

References

- Agnini, C., Macri, P., Backman, J., Brinkhuis, H., Fornaciari, E., Giusberti, L., Luciani, V., Rio, D., Sluijs, A., and Speranza, F., 2009. An early Eocene carbon cycle perturbation at ~52.5 Ma in the Southern Alps: chronology and biotic response. *Paleoceanography*, 24(2):PA2209. doi:10.1029/2008PA001649
- Brotzen, F., 1948. The Swedish Paleocene and its foraminiferal fauna. *Arsb. Sver. Geol. Unders.*, Ser. C, 493:1–140.
- Cushman, J.A., 1946. Upper Cretaceous foraminifera of the Gulf Coastal region of the United States and adjacent areas. *U.S. Geol. Surv. Prof. Pap.*, 206:1–241.
- Cushman, J.A., 1951. Paleocene foraminifera of the Gulf Coastal region of the United States and adjacent areas. *U.S. Geol. Surv. Prof. Pap.*, 232:1–75.
- Cushman, J.A., and Jarvis, P.W., 1932. Upper Cretaceous foraminifera from Trinidad. *Proc. U.S. Nat. Mus.*, 80:1–60.
- D'haenens, S., Bornemann, A., Stassen, P., and Speijer, R.P., 2012. Multiple early Eocene benthic foraminiferal assemblage and $\delta^{13}\text{C}$ fluctuations at DSDP Site 401 (Bay of Biscay—NE Atlantic). *Mar. Micropaleontol.*, 88–89:15–35. doi:10.1016/j.marmicro.2012.02.006
- Gooday, A.J., 2003. Benthic foraminifera (Protista) as tools in deep-water paleoceanography: environmental influences on faunal characteristics. *Adv. Mar. Biol.*, 46:1–90. doi:10.1016/S0065-2881(03)46002-1
- Griffith, E., Calhoun, M., Thomas, E., Averyt, K., Erhardt, A., Bralower, T., Lyle, M., Olivarez-Lyle, A., and Paytan, A., 2010. Export productivity and carbonate accumulation in the Pacific Basin at the transition from a greenhouse to icehouse climate (late Eocene to early Oligocene). *Paleoceanography*, 25(3):PA3212. doi:10.1029/2010PA001932
- Jones, R.W., 1994. *The Challenger Foraminifera*: New York (Oxford).
- Kaminski, M.A., and Gradstein, F.M., 2005. Atlas of Paleogene cosmopolitan deep-water agglutinated foraminifera. *Grzybowski Found. Spec. Publ.*, 10. <http://www.foraminifera.eu/atlas.html>
- Kennett, J.P., and Stott, L.D., 1991. Abrupt deep-sea warming, paleoceanographic changes and benthic extinctions at the end of the Palaeocene. *Nature (London, U. K.)*, 353(6341):225–229. doi:10.1038/353225a0
- Loeblich, A.R., Jr., and Tappan, H., 1988. *Foraminiferal Genera and Their Classification*: New York (Van Nostrand Reinhold).
- Lourens, L.J., Sluijs, A., Kroon, D., Zachos, J.C., Thomas, E., Röhl, U., Bowles, J., and Raffi, I., 2005. Astronomical pacing of late Palaeocene to early Eocene global warming events. *Nature (London, U. K.)*, 435(7045):1083–1087. doi:10.1038/nature03814
- Lyle, M., Olivarez Lyle, A., Backman, J., and Tripathi, A., 2005. Biogenic sedimentation in the Eocene equatorial Pacific—the stuttering greenhouse and Eocene carbonate compensation depth. In Lyle, M., Wilson, P.A., Janecek, T.R., et al., *Proc. ODP, Init. Repts.*, 199: College Station, TX (Ocean Drilling Program), 1–35. doi:10.2973/odp.proc.sr.199.219.2005
- Nomura, R., and Takata, H., 2005. Data report: Paleocene/Eocene benthic foraminifers, ODP Leg 199 Sites 1215, 1220, and 1221, equatorial central Pacific Ocean. In Wilson, P.A., Lyle, M., and Firth, J.V. (Eds.), *Proc. ODP, Sci. Results*, 199: College Station, TX (Ocean Drilling Program), 1–34. doi:10.2973/odp.proc.sr.199.223.2005
- Pälike, H., Nishi, H., Lyle, M., Raffi, I., Klaus, A., Gamage, K., and the Expedition 320/321 Scientists, 2009. Pacific Equatorial Age Transect. *IODP Prel. Rept.*, 320. doi:10.2204/iodp.pr.320.2009
- Plummer, H.J., 1926. Foraminifera of the Midway formation in Texas. *Texas Univ. Bull.*, 2644.
- Shipboard Scientific Party, 2002. Leg 199 summary. In Lyle, M., Wilson, P.A., Janecek, T.R., et al., *Proc. ODP, Init. Repts.*, 199: College Station, TX (Ocean Drilling Program), 1–87. doi:10.2973/odp.proc.ir.199.101.2002
- Stap, L., Lourens, L.J., Thomas, E., Sluijs, A., Bohaty, S., and Zachos, J.C., 2010. High-resolution deep-sea carbon and oxygen isotope records of Eocene Thermal Maximum 2 and H2. *Geology*, 38(7):607–610. doi:10.1130/G30777.1
- Thomas, E., 2007. Cenozoic mass extinctions in the deep sea: what disturbs the largest habitat on Earth? In Monechi, S., Coccioni, R., and Rampino, M. (Eds.), *Large Ecosystem Perturbations: Causes and Consequences*. Spec. Pap.—Geol. Soc. Am., 424:1–23. doi:10.1130/2007.2424(01)
- Tjalsma, R.C., and Lohmann, G.P., 1983. Paleocene–Eocene bathyal and abyssal benthic foraminifera from the Atlantic Ocean. *Micropaleontology, Spec. Publ.*, 4.

- van Morkhoven, F.P.C.M., Berggren, W.A., Edwards, A.S., and Oertli, H.J., 1986. Cenozoic cosmopolitan deep-water benthic foraminifera. *Bull. Cent. Rech. Explor.—Prod. Elf-Aquitaine*, 11.
- Westerhold, T., Röhl, U., Wilkens, R., Pälike, H., Lyle, M., Jones, T.D., Bown, P., Moore, T., Kamikuri, S., Acton, G., Ohneiser, C., Yamamoto, Y., Richter, C., Fitch, P., Scher, H., Liebrand, D., and the Expedition 320/321 Scientists, 2012. Revised composite depth scales and integration of IODP Sites U1331–U1334 and ODP Sites 1218–1220. In Pälike, H., Lyle, M., Nishi, H., Raffi, I., Gamage, K., Klaus, A., and the Expedition 320/321 Scientists, *Proc. IODP, 320/321: Tokyo (Integrated Ocean Drilling Program Management International, Inc.)*. doi:10.2204/iodp.proc.320321.201.2012
- Winguth, A.M.E., Thomas, E., and Winguth, C., 2012. Global decline in ocean ventilation, oxygenation, and productivity during the Paleocene-Eocene Thermal Maximum: implications for the benthic extinction. *Geology*, 40(3):263–266. doi:10.1130/G32529.1
- Zachos, J.C., McCarren, H., Murphy, B., Röhl, U., and Westerhold, T., 2010. Tempo and scale of late Paleocene and early Eocene carbon isotope cycles: implications for the origin of hyperthermals. *Earth Planet. Sci. Lett.*, 299(1–2):242–249. doi:10.1016/j.epsl.2010.09.004
- Initial receipt:** 30 July 2012
Acceptance: 25 March 2013
Publication: 17 October 2013
MS 320321-212

Appendix

Faunal reference list

Agglutinated foraminifers

Ammobaculites sp.

Ammovertellina prima Suleymanov, 1959 (Pl. **P1**, fig. 9).

Bathysiphon sp.

Cyclammina elegans Cushman and Jarvis, 1928 (Pl. **P1**, fig. 5).

Gaudryina retusa Cushman, 1926 (Pl. **P1**, fig. 1).

Gaudryina sp.

Karrieriella sp.

Karrieriella subglabra (Cushman) (Pl. **P1**, fig. 3) = *Gaudryina subglabra* Gümbel, 1868.

Marssonella trochoides (d'Orbigny) (Pl. **P1**, fig. 2) = *Gaudryina crassa* Marsson var. *trochoides* Marsson, 1878.

Paratrochamminoides olszewskii (Grzybowski) (Pl. **P1**, figs. 6, 7) = *Trochammina olszewski* Grzybowski, 1898.

Psammosiphonella cylindrica (Glaessner) (Pl. **P1**, fig. 4) = *Rhabdammina cylindrica* Glaessner, 1937.

Spiroplectammmina spectabilis (Grzybowski) (Pl. **P2**, fig. 1) = *Spiroplecta spectabilis* Grzybowski, 1898.

Textularia plummerae Lalicker, 1935 (Pl. **P9**, fig. 1).

Textularia sp.

Thalmanammmina conglobata (Brady) (Pl. **P1**, fig. 11) = *Trochammina conglobata* Brady, 1884.

Tritaxia globulifera (ten Dam and Sigal) (Pl. **P1**, figs. 12, 13) = *Pseudoclavulina globulifera* ten Dam and Sigal, 1950.

Tritaxia paleocenica Tjalsma and Lohmann, 1983.

Tritaxia pyramidata (Cushman) = *Gaudryina laevigata* Franke var. *pyramidata* Cushman, 1926.

Vulvulina spinosa Cushman, 1927 (Pl. **P2**, figs. 2–4).

Calcareous hyaline foraminifers

Abyssamina quadrata Schnitker and Tjalsma, 1980 (Pl. **P5**, figs. 4, 5).

Alabamina dissonata (Cushman and Renz) (Pl. **P8**, figs. 6–8) = *Pulvinulinella atlantisae* Cushman var. *dissonata* Cushman and Renz, 1948.

Amplectoproductina carnatolintra Patterson, 1986 (Pl. **P4**, figs. 16, 17).

Anomalinoides rubiginosus (Cushman) (Pl. **P6**, figs. 4, 5) = *Anomalina rubiginosa* Cushman, 1926.

Anomalinoides spissiformis (Cushman and Stainforth) (Pl. **P6**, figs. 1–3) = *Anomalina alazanensis* Nuttall var. *spissiformis* Cushman and Stainforth, 1945.

Aragonina aragonensis (Nuttall) (Pl. **P5**, fig. 19) = *Textularia aragonensis* Nuttall, 1930.

Bandyella greatvalleyensis (Trujillo) (Pl. **P4**, figs. 8, 9, 13) = *Pleurostomella greatvalleyensis* Trujillo, 1960.

Bulimina bradburyi Martin, 1943.

Bulimina impendens Parker and Bermudez, 1937 (Pl. **P9**, fig. 5).

Bulimina jarvisi Cushman and Parker, 1936 (Pl. **P5**, fig. 15).

Bulimina tuxpamensis Cole, 1928 (Pl. **P5**, figs. 8, 9).

Buliminella beaumonti Cushman and Renz, 1946 (Pl. **P5**, figs. 10, 11).

Cibicoides bradyi (Trauth) (Pl. **P7**, fig. 6) = *Truncatulina bradyi* Trauth, 1918.

Cibicoides eocaenus (Gümbel) (Pl. **P7**, figs. 4, 5) = *Rotalia eocaena* Gümbel, 1868.

Cibicoides grimsdalei (Nuttall) (Pl. **P7**, figs. 1–3) = *Cibicides grimsdalei* Nuttall, 1930.

Cibicoides spp.

Clinapertina inflata Tjalsma and Lohmann, 1983 (Pl. **P9**, fig. 9).

Clinapertina subplanispira Tjalsma and Lohmann, 1983 (Pl. **P9**, fig. 10).

Coryphostoma crenulata (Cushman) (Pl. **P5**, fig. 7) = *Bolivina crenulata* Cushman, 1936.

Dentalina annulata (Reuss) = *Nodosaria annulata* Reuss, 1844.

Dentalina guttifera d'Orbigny, 1846 (Pl. **P3**, fig. 12).

Dentalina reflexa Morrow, 1934 (Pl. **P3**, figs. 5, 6).

Dentalina spp.

Dentalina subsoluta (Cushman) = *Nodosaria subsoluta* Cushman, 1923.

Ellipsoglandulina ovata Gawor-Biedowa, 1992 (Pl. **P4**, fig. 18).

Ellipsoidella pleurostomelloides Heron-Allen and Earland, 1910 (Pl. **P2**, fig. 7; Pl. **P4**, Fig. 12).

Ellipsopolymorphina sp. (Pl. **P2**, fig. 14).

Ellipsopolymorphina spp.

Eouvigerina hispida Cushman, 1931 (Pl. **P9**, fig. 2).

Glandulonodosaria ambigua (Neugeboren) (Pl. **P3**, fig. 4) = *Nodosaria ambigua* Neugeboren, 1856.

Globocassidulina globosa (Hantken) (Pl. **P5**, figs. 17, 18) = *Cassidulina globosa* Hantken, 1875.

Globulina gibba (d'Orbigny) (Pl. **P2**, fig. 5) = *Polymorphina gibba* d'Orbigny, 1826.

Gyroidinoides beisseli (White) = *Gyroidina beisseli* White, 1928.

- Gyroidinoides girardanus* (Reuss) (Pl. P8, fig. 5) = *Rotalina girardana* Reuss, 1851.
- Gyroidinoides* cf. *globosus* (Hagenow) (Pl. P8, fig. 4) = cf. *Nonionia globosa* Von Hagenow, 1842.
- Gyroidinoides* spp.
- Hemirobulina* sp.
- Heronallenia lingulata* (Burrows and Holland) (Pl. P5, fig. 20) = *Discorbina lingulata* Burrow and Holland, 1895.
- Lenticulina insulsus* (Cushman) (Pl. P6, fig. 10) = *Robulus insulsus* Cushman, 1947.
- Lenticulina* spp. (Pl. P6, fig. 11).
- Linaresia semicribrata* (Beckmann) = *Anomalina pompilioides* Galloway and Hemingway var. *semicribrata* Beckmann, 1954.
- Marginulina glabra* d'Orbigny, 1826 (Pl. P2, fig. 10).
- Marginulina* sp. (Pl. P2, fig. 9).
- Marginulinopsis* sp.
- Nodogenerina* sp.
- Nodosarella rotundata* (D'Orbigny) (Pl. P2, fig. 6) = *Lingulina rotundata* d'Orbigny, 1846.
- Nodosarella tuberosa* (Gümbel) (Pl. P3, fig. 7; Pl. P4, fig. 15) = *Lingulina tuberosa* Gümbel, 1868.
- Nodosaria annulata* Reuss, 1844 (Pl. P3, fig. 11).
- Nodosaria jarvisi* (Cushman) (Pl. P3, fig. 3) = *Ellipsonodosaria* ? *jarvisi* Cushman, 1936.
- Nodosaria naumanni* Reuss (Pl. P3, fig. 1) = *Nodosaria* (*Nodosaria*) *naumanni* Reuss, 1875.
- Nodosaria* spp.
- Nodosaria velascoensis* Cushman (Pl. P3, fig. 2) = *Nodosaria fontannesii* Berthelin var. *velascoensis* Cushman, 1926.
- Nonion havanense* Cushman and Bermudez, 1937 (Pl. P5, fig. 16).
- Nonion* spp.
- Nuttallides truempyi* (Nuttall) (Pl. P8, figs. 1–3) = *Eponides truempyi* Nuttall, 1930.
- Obliquilingulina oblonga* Zheng, 1979 (Pl. P2, fig. 15).
- Oridorsalis plummerae* (Cushman) (Pl. P2, fig. 11) = *Eponides plummerae* Cushman, 1948.
- Oridorsalis umbonatus* (Reuss) (Pl. P8, figs. 9–11) = *Rotalina umbonata* Reuss, 1851.
- Orthomorphina havanensis* (Cushman and Bermudez) (Pl. P4, fig. 10) = *Nodogenerina havanensis* Cushman and Bermudez, 1937.
- Orthomorphina* sp.
- Osangularia plummerae* Brotzen, 1940 (Pl. P5, figs. 1–3).
- Paralabamina elevata* (Plummer) (Pl. P9, fig. 8) = *Truncatulinina elevata* Plummer, 1927.
- Pleurostomella clavata* Cushman, 1926 (Pl. P2, fig. 8).
- Pleurostomella subnodosa* Reuss, 1860 (Pl. P4, fig. 14).
- Pseudonodosaria appressa* (Loeblich and Tappan) (Pl. P3, figs. 9, 10) = *Rectoglandulina appressa* Loeblich and Tappan, 1955.
- Pseudonodosaria obesa* (Loeblich and Tappan) (Pl. P3, fig. 8) = *Rectoglandulina obesa* Loeblich and Tappan, 1955.
- Pullenia* cf. *eocenica* Cushman and Siegfus, 1939.
- Pullenia coryelli* White, 1929 (Pl. P6, figs. 6, 7).
- Pullenia cretacea* Cushman, 1936 (Pl. P9, fig. 4).
- Pullenia jarvisi* Cushman, 1936 (Pl. P6, figs. 8, 9).
- Pullenia* sp.
- Pyrulina* sp.
- Pyrulinoidea acuminatus* (d'Orbigny) (Pl. P2, fig. 13) = *Pyrulina acuminata* d'Orbigny, 1840.
- Quadratobuliminella pyramidalis* de Klasz, 1953 (Pl. P5, figs. 12–14).
- Saracenaria midwayensis* Kline, 1943 (Pl. P2, fig. 12).
- Siphonodosaria aculeata* (Cushman and Renz) (Pl. P4, figs. 2–5) = *Ellipsonodosaria nuttalli* var. *aculeata* Cushman and Renz, 1948.
- Stilostomella gracillima* (Cushman and Jarvis) (Pl. P4, fig. 7) = *Ellipsonodosaria nuttalli* var. *gracillima* Cushman and Jarvis, 1934.
- Stilostomella hispidula* (Cushman) (Pl. P4, fig. 6) = *Ellipsonodosaria atlantisae* var. *hispidula* Cushman, 1939.
- Stilostomella jacksonensis* (Cushman and Applin) (Pl. P4, fig. 1) = *Nodosaria jacksonensis* Cushman and Applin, 1926.
- Strictocostella prolata* (Cushman and Bermudez) (Pl. P4, fig. 11) = *Ellipsonodosaria modesta* var. *prolata* Cushman and Bermudez, 1937.
- Tappanina selmensis* (Cushman) (Pl. P9, fig. 6) = *Bolivina selmensis* Cushman, 1933.
- Valvalabamina depressa* (Alth) (Pl. P9, fig. 7) = *Rotalina depressa* Alth, 1850.
- Valvulineria* spp.
- Virgulinopsis navarroana* (Cushman) (Pl. P5, fig. 6) = *Virgulinina navarroana* Cushman, 1933.
- Unilocular forms

Figure F1. Site map for DSDP, ODP, and IODP in the equatorial central Pacific Ocean. F.Z. = fracture zone.

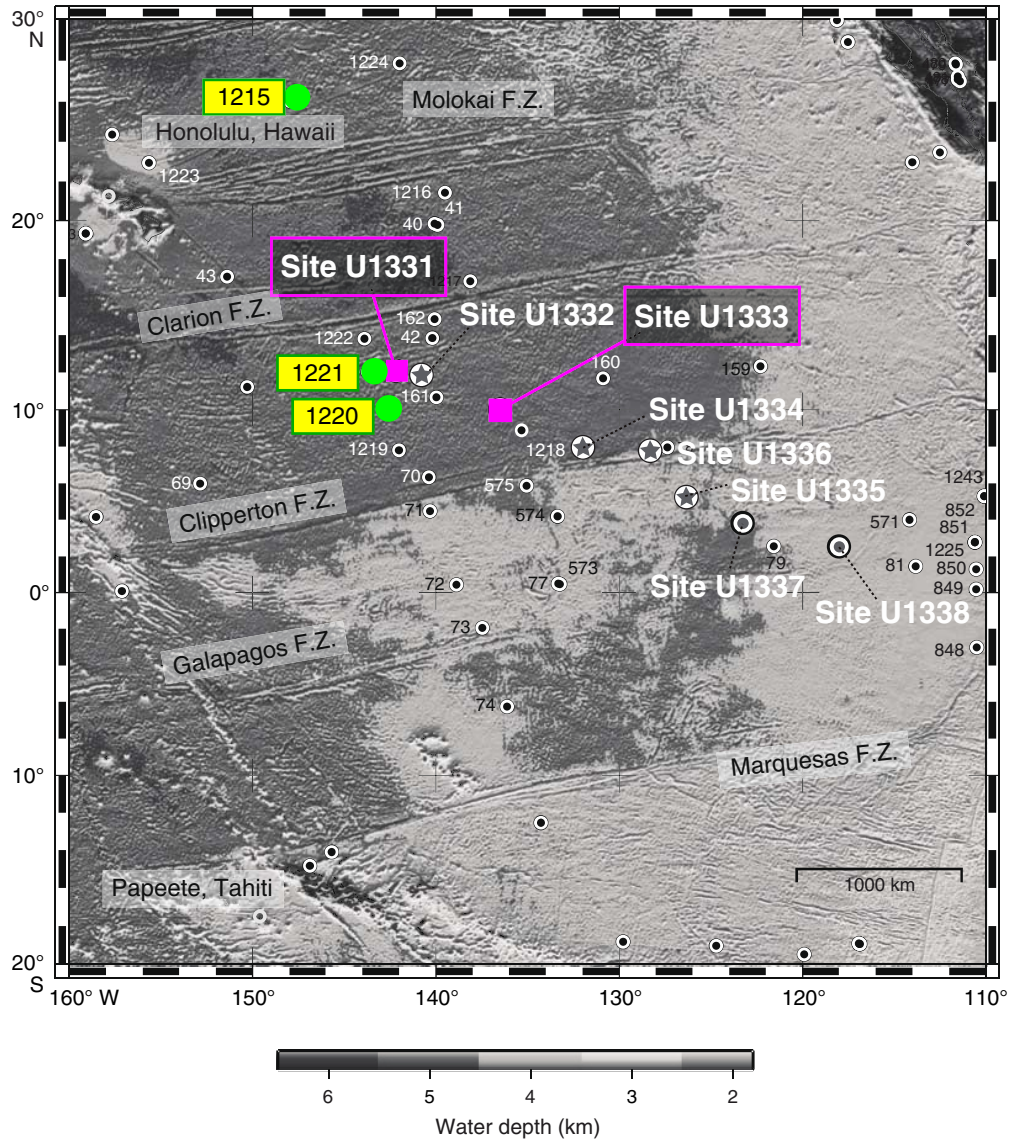


Figure F2. Benthic foraminiferal occurrences. Arrows indicate the marked stratigraphic levels of the foraminiferal assemblage.

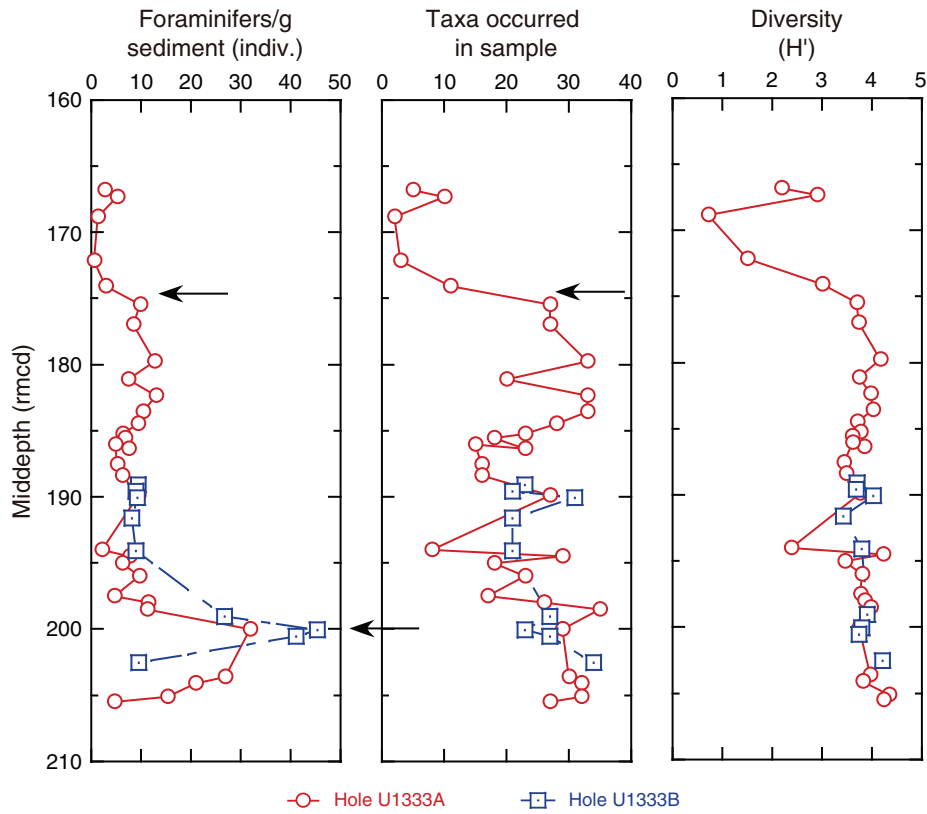


Plate P1. Horizontal scale bar = 200 μm . Vertical scale bar = 400 μm . 1–3. Sample 320-1333A-17X-4, 75–77 cm; (1) *Gaudryina retusa* Cushman, (2) *Marssonella trochoides* (Marsson), (3) *Karriella subglabra* (Gümbel). 4. *Psamosiphonella cylindrica* (Glaessner) (Sample 320-U1331C-17H-3, 128–130 cm). 5–7. Sample 320-1331C-17H-4, 28–30 cm; (5) *Cyclammina elegans* Cushman and Jarvis, (6, 7) *Paratrochamminoides olszewskii* (Grzybowski). 8. *Gaudryina pyramidata* Cushman (Sample 320-U1333A-20X-2, 25–27 cm). 9. *Ammovertellina prima* Suleymanov (Sample 320-U1331C-17H-3, 128–130 cm). 10. *Tritaxia havanensis* (Cushman and Bermudez) (Sample 320-U1333B-19X-3, 23–25 cm). 11. *Thalmanammina conglobata* (Brady) (Sample 320-U1331C-17H-3, 128–130 cm). 12, 13. *Tritaxia globulifera* (ten Dam and Sigal); (12) Sample 320-U1333A-20X-2, 65–67 cm, (13) Sample 320-U1331C-17H-3, 128–130 cm.

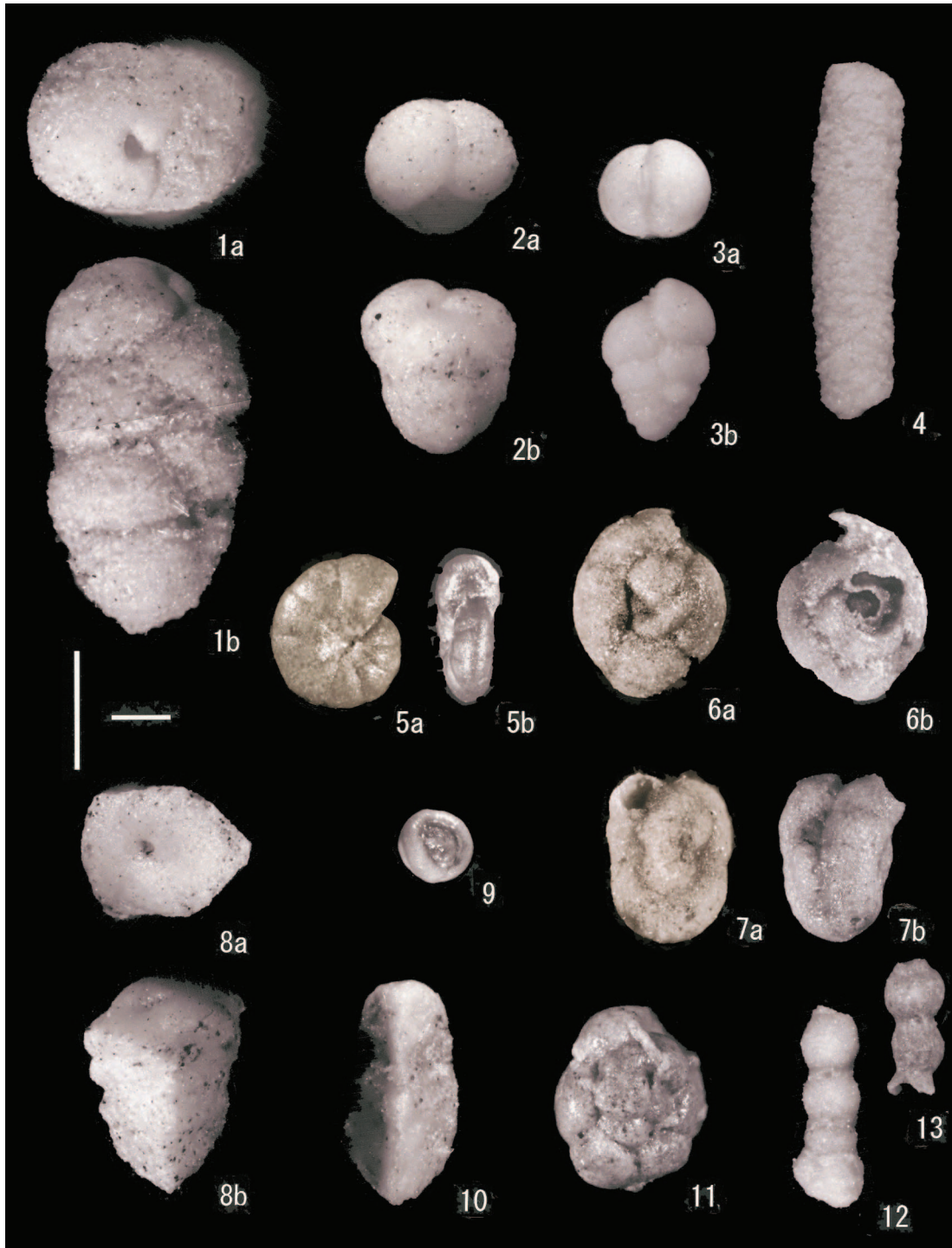


Plate P2. Horizontal scale bar = 200 μm . Vertical scale bar = 400 μm . 1. *Spiroplectammina spectabilis* (Grybowski) (Sample 320-1333A-17X-1, 75–77 cm). 2–4. *Vulvulina spinosa* Cushman; (2) Sample 320-U1333B-19X-3, 23–25 cm, (3) Sample 320-U1333A-17X-7, 25–27 cm, (4) Sample 320-U1333A-18X-4, 75–77 cm. 5. *Globulina gibba* d'Orbigny (Sample 320-U1333A-17X-1, 75–77 cm). 6. *Nodosarella rotundata* (d'Orbigny) (Sample 320-1333A-U17X-7, 25–27 cm). 7. *Ellipsoidella pleurostomelloides* Heron-Allen and Earland (Sample 320-U1333A-18X-4, 75–77 cm). 8. *Pleurostomella clavata* Cushman (Sample 320-U1333A-18X-4, 75–77 cm). 9. *Marginulina* sp. (Sample 320-U1333A-20X-2, 25–27 cm). 10. *Marginulina glabra* d'Orbigny (Sample 320-U1333B-19X-2, 23–25 cm). 11. *Oridorsalis plummerae* (Cushman) (Sample 320-U1333B-19X-3, 123–125 cm). 12. *Saracenaria midwayensis* Kline (Sample 320-U1333B-19X-2, 123–125 cm). 13. *Pyrulinoidea acuminatus* (d'Orbigny) (Sample 320-U1333A-17X-6, 25–27 cm). 14. *Ellipsopolymorphina* sp. (Sample 320-U1331C-17H-3, 78–80 cm). 15. *Obliquilina oblonga* Zheng (Sample 320-U1331C-17H-3, 78–80 cm).



Plate P3. Horizontal scale bar = 200 μm . Vertical scale bar = 400 μm . 1. *Nodosaria naumanni* Reuss (Sample 320-U1333A-19X-4, 25–27 cm). 2. *Nodosaria velascoensis* Cushman (Sample 320-U1333A-19X-4, 25–27 cm). 3. *Nodosaria jarvisi* (Cushman) (Sample 320-U1333A-17X-7, 25–27 cm). 4. *Glandulonodosaria ambigua* (Neugeboren) (Sample 320-U1333A-19X-5, 25–27 cm). 5, 6. *Dentalina reflexa* Morrow; (5) Sample 320-U1333A-17X-1, 75–77 cm, (6) Sample 320-U1333A-17X-1, 75–77 cm. 7. *Nodosarella tuberosa* (Gümbel) (Sample 320-U1333A-17X-1, 75–77 cm). 8. *Pseudonodosaria obesa* (Loeblich and Tappan) (Sample 320-U1333A-17X-7, 25–27 cm). 9, 10. *Pseudonodosaria appressa* (Loeblich and Tappan); (9) Sample 320-U1333B-20X-3, 123–125 cm, (10) Sample 320-U1333A-17X-7, 25–27 cm. 11. *Nodosaria annulata* Reuss (Sample 320-U1333A-20X-2, 25–27 cm). 12. *Dentalina guttifera* d'Orbigny (Sample 320-U1333B-19X-3, 23–25 cm).



Plate P4. Horizontal scale bar = 200 μm . Vertical scale bar = 400 μm . 1. *Stilostomella jacksonensis* (Cushman and Applin) (Sample 320-U1333A-19X4, 25–27 cm). 2–5. *Siphonodosaria aculeata* (Cushman and Renz); (2–4) Sample 320-U1333A-19X-4, 25–27 cm, (5) Sample 320-U1333A-20X-2, 65–67 cm. 6. *Stilostomella hispidula* (Cushman) (Sample 320-U1333A-17X-4, 75–77 cm). 7. *Stilostomella gracillima* (Cushman and Jarvis) (Sample 320-U1333A-17X-7, 25–27 cm). 8, 9, 13. *Bandyella greatvalleyensis* (Trujillo); (8) Sample 320-U1333A-19X-4, 25–27 cm, (9) Sample 320-U1333A-19X-4, 25–27 cm, (13) Sample 320-U1333A-17X-1, 75–77 cm. 10. *Orthomorphina havanensis* (Cushman and Bermudez) (Sample 320-U1333A-20X-2, 65–67 cm). 11. *Strictocostella prolata* (Cushman and Bermudez) (Sample 320-U1333A-20X-2, 65–67 cm). 12. *Ellipsooidella pleurostomeloides* Heron-Allen and Earland (Sample 320-U1333A-20X-1, 75–77 cm). 14. *Pleurostomella subnodosa* Reuss (Sample 320-U1333A-17X-1, 75–77 cm). 15. *Nodosarella tuberosa* (Gümbel) (Sample 320-U1333A-20X-2, 65–67 cm). 16, 17. *Amplectoproductina carnatintra* Patterson (Sample 320-U1333A-18X-4, 75–77 cm). 18. *Ellipso-glandulina ovata* Gawor-Biedowa (Sample 320-U1333A-19X-4, 25–27 cm).

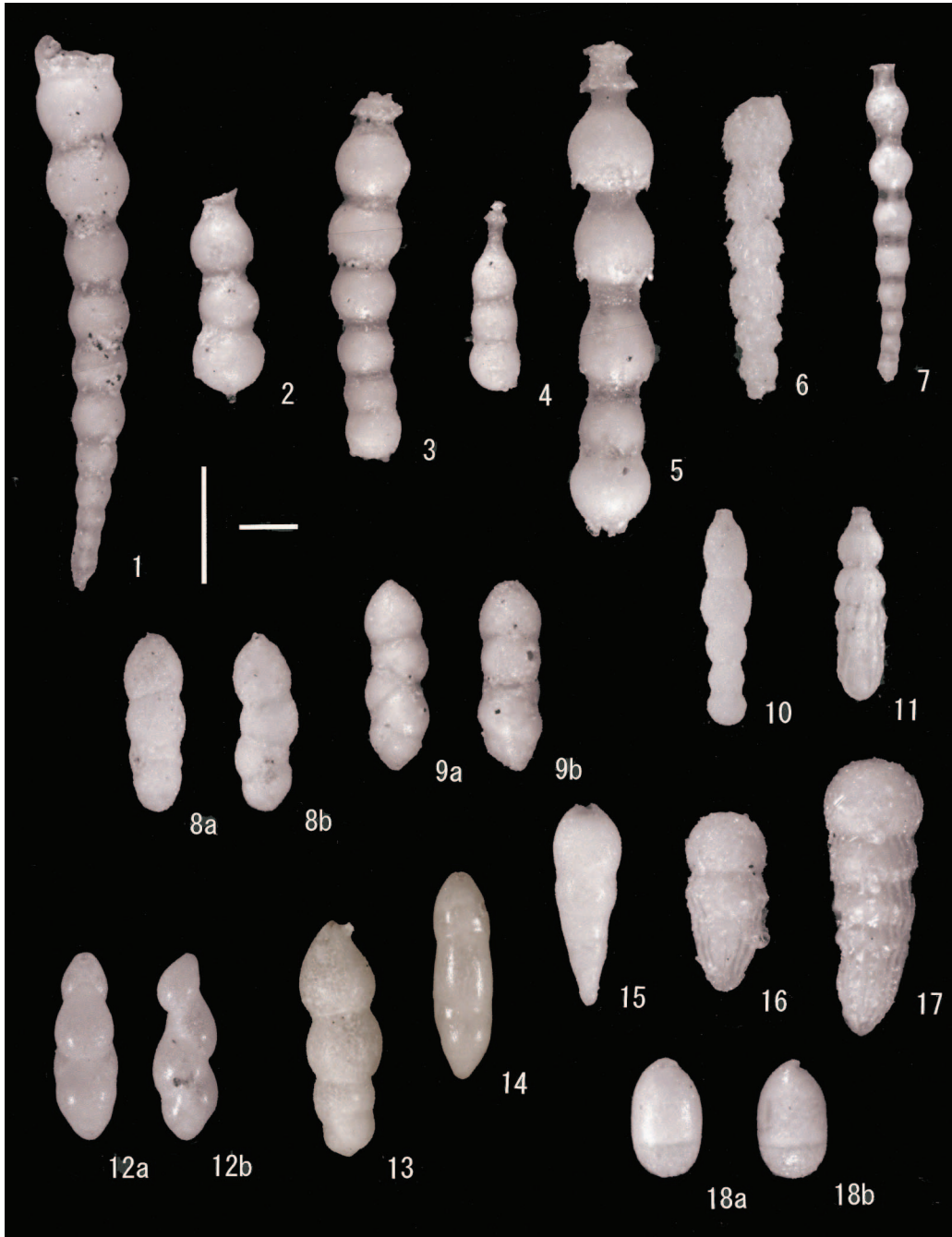


Plate P5. Horizontal scale bar = 200 μm . Vertical scale bar = 400 μm . 1–3. *Osangularia plummerae* Brotzen (Sample 320-U1333A-17X-1, 75–77 cm). 4, 5. *Abyssamina quadrata* Schnitker and Tjalsma; (4) Sample 320-U1333A-20X-1, 75–77 cm, (5) Sample 320-U1333A-18X-4, 75–77 cm. 6. *Virgulinoopsis navarroanus* (Cushman) (Sample 320-U1333A-17X-4, 75–77 cm). 7. *Coryphostoma crenulata* (Cushman) (Sample 320-U1333B-20X-3, 123–125 cm). 8, 9. *Bulimina tuxpamensis* Cole; (8) Sample 320-U1333B-19X-1, 123–125 cm, (9) Sample 320-U1331C-17H-3, 78–80 cm. 10, 11. *Buliminella beaumonti* Cushman and Renz; (10) Sample 320-U1333B-20X-2, 23–25 cm, (11) Sample 320-U1333B-20X-3, 123–125 cm. 12–14. *Quadratobuliminella pyramidalis* de Klasz; (12) Sample 320-U1333B-20X-3, 123–125 cm, (13) Sample 320-U1331C-17H-3, 78–80 cm, (14) Sample 320-U1333A-20X-2, 25–27 cm. 15. *Bulimina jarvisi* Cushman and Parker (Sample 320-U1333A-20X-1, 75–77 cm). 16. *Nonion havanense* Cushman and Bermudez (Sample 320-U1333A-20X-2, 65–67 cm). 17, 18. *Globocassidulina globosa* Hantken; (17) Sample 320-U1333A-19X-4, 25–27 cm, (18) Sample 320-U1333B-20X-2, 23–25 cm. 19. *Aragonia aragonensis* (Nuttall) (Sample 320-U1333A-20X-1, 75–77 cm). 20. *Heronallenia lingulata* (Burrows and Holland) (Sample 320-U1333A-20X-1, 75–77 cm).



Plate P6. Horizontal scale bar = 200 μm . Vertical scale bar = 400 μm . 1–3. *Anomalinoides spissiformis* (Cushman and Stainforth); (1) Sample 320-U1333A-20X-2, 25–27 cm, (2, 3) Sample 320-U1333A-17X-4, 75–77 cm. 4, 5. *Anomalinoides rubiginosus* (Cushman); (4) Sample 320-U1333A-20X-1, 75–77 cm, (5) Sample 320-U1333A-17X-7, 25–27 cm. 6, 7. *Pullenia coryelli* White; (6) Sample 320-U1333B-20X-2, 23–25 cm, (7) Sample 320-U1333A-17X-7, 25–27 cm. 8, 9. *Pullenia jarvisi* Cushman; (8) Sample 320-U1333A-18X-4, 75–77 cm, (9) Sample 320-U1333A-17X-1, 75–77 cm. 10. *Lenticulina insulsus* Cushman of Plummer (Sample 320-U1333A-20X-2, 65–67 cm). 11. *Lenticulina* sp. (Sample 320-U1333A-20X-1, 75–77 cm).



Plate P7. Horizontal scale bar = 200 μm . Vertical scale bar = 400 μm . 1–3. *Cibicidoides grimsdalei* (Nuttall); (1, 3) Sample 320-U1333A-18X-4, 75–77 cm, (2) Sample 320-U1333B-19X-2, 23–25 cm. 4, 5. *Cibicidoides eo-caenus* (Gümbel); (4) Sample 320-U1333A-18X-4, 75–77 cm, (5) Sample 320-U1333A-20X-1, 75–77 cm. 6. *Cibicidoides bradyi* (Trauth) (Sample 320-U1333A-17X-7, 25–27 cm.)

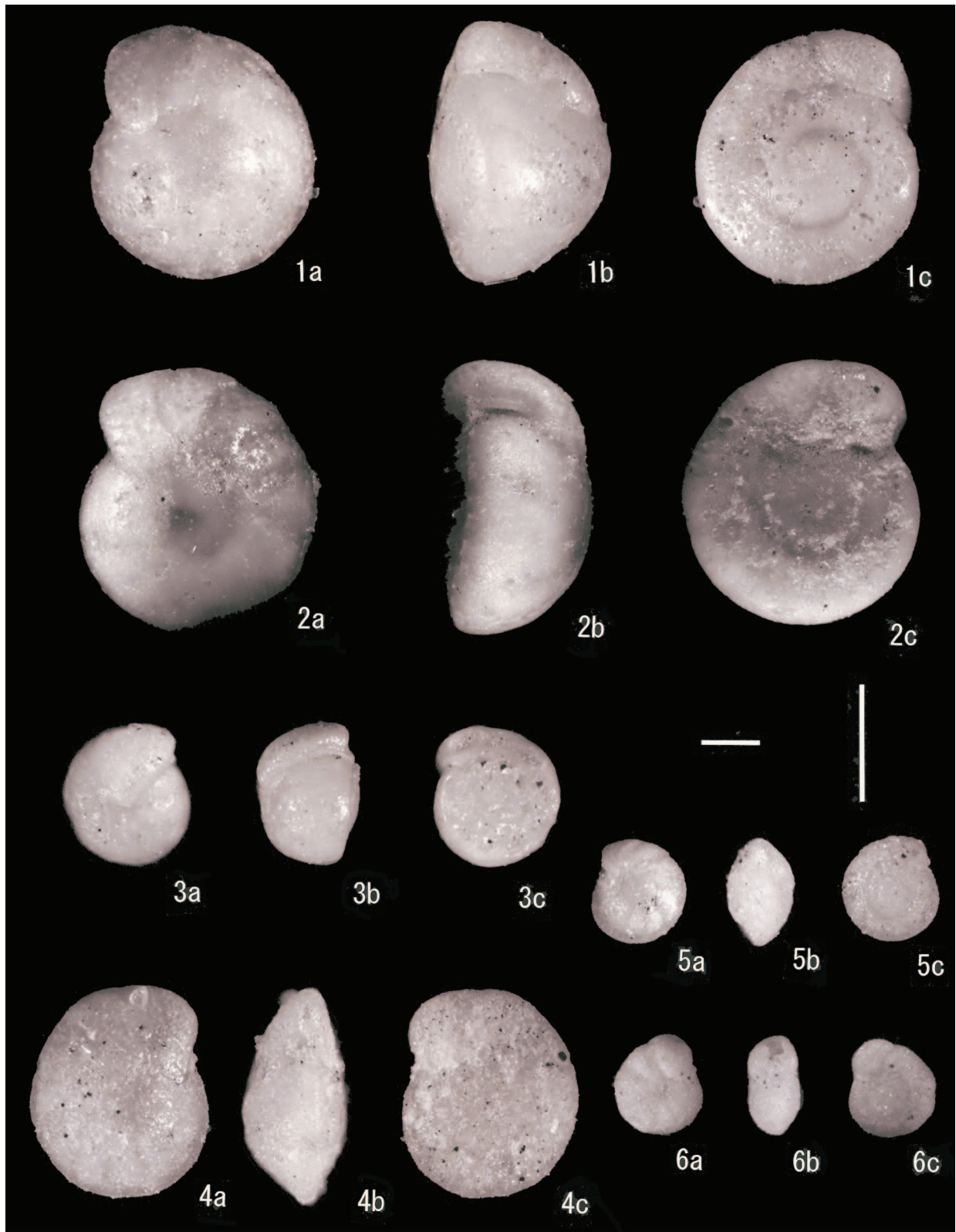


Plate P8. Horizontal scale bar = 200 μm . Vertical scale bar = 400 μm . 1–3. *Nuttallides truempyi* (Nuttall); (1) Sample 320-U1333A-17X-4, 75–77 cm, (2, 3) Sample 320-U1333A-17X-1, 75–77 cm. 4. *Gyroidinoides* cf. *globosus* (Hagenow) (Sample 320-U1333A-17X-1, 75–77 cm). 5. *Gyroidinoides girardanus* (Reuss) (Sample 320-U1333A-17X-4, 75–77 cm). 6–8. *Alabamina dissonata* (Cushman and Renz); (6, 7) Sample 320-U1333B-19X-2, 23–25 cm, (8) Sample 320-U1333A-17X-4, 75–77 cm. 9–11. *Oridorsalis umbonatus* (Reuss); (9, 10) Sample 320-U1333A-17X-4, 75–77 cm, (11) Sample 320-U1333B-19X-2, 23–25 cm.

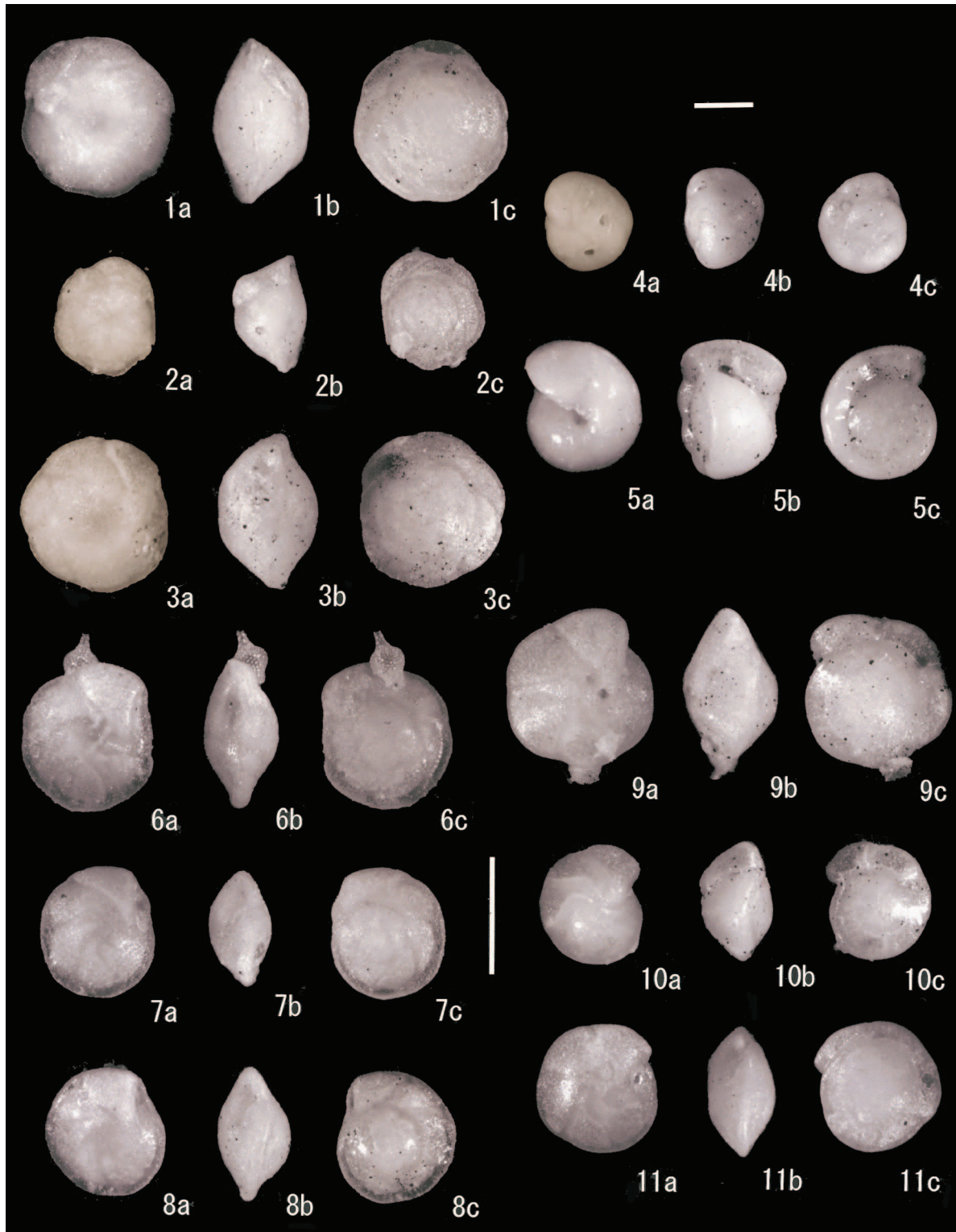


Plate P9. Horizontal scale bar = 200 μm . Vertical scale bar = 400 μm . 1. *Textularia plummerae* Lalicker (Sample 320-U1333A-19X-5, 25–27 cm). 2. *Eouvigerina hispida* Cushman (Sample 320-U1333A-18X-2, 75–77 cm). 3. *Stilostomella* sp. (Sample 320-U1333B-19X-2, 123–125 cm). 4. *Pullenia cretacea* Cushman (Sample 320-U1333B-19X-2, 23–25 cm). 5. *Bulimina impendens* Parker and Bermudez (Sample 320-U1333A-20X-2, 25–27 cm). 6. *Tappanina selmensis* (Cushman) (Sample 320-U1331C-17H-3, 78–80 cm). 7. *Valvalabamina depressa* (Alth) (Sample 320-U1333B-20X-3, 123–125 cm). 8. *Paralabamina elevata* (Plummer) (Sample 320-U1333B-19X-1, 73–75 cm). 9. *Clinapertina inflata* Tjalsma and Lohmann (Sample 320-U1333B-20X-3, 123–125 cm). 10. *Clinapertina subplanipecta* Tjalsma and Lohmann (Sample 320-U1331C-17H-3, 78–80 cm).

